EAST EUROPEAN JOURNAL OF PHYSICS. 3. 608-616 (2026)
DOI:10.26565/2312-4334-2026-3-56 ISSN 2312-4334

LATERAL PHOTOEFFECT IN METAL–OXIDE–SEMICONDUCTOR STRUCTURES BASED ON MONOCRYSTALLINE SILICON

E.U. Arzikulov[1,2]*, R.M. Usanov[1], Sh.J. Quvondiqov[1], Teng Lui[1,2], D.T. Bobonov[3], S.A. Sattarov[1,3]

[1]*Samarkand State University named after Sharof Rashidov, 140001, University blv. 15, Samarkand, Uzbekistan*
[2]*School of Material Science and Engineering, Shenyang Aerospace University, 37 Daoyi South Avenue, Shenyang, China*
[3]*Jizzakh Polytechnic Institute, Jizzakh, Uzbekistan*
**Corresponding author email: eshkuvata@gmail.com*
Received June 10, 2026; revised August 10, 2026; accepted August 26, 2026

This paper presents the fabrication technology and experimental results of the lateral photoeffect (LPE) study in Co/SiO₂/n-Si⟨P, Zn⟩ metal-oxide-semiconductor (MOS) structures. The structures were prepared based on initial n-type silicon samples (ρ=1.05 Ω×cm), thermally annealed samples (ρ=1.07 Ω×cm), and highly Zn-compensated n-type silicon samples with specific resistivities of 5.04 Ω×cm, 156.86 Ω×cm, and 1800 Ω×cm, respectively. According to the experimental results, the dependence of the lateral photovoltage (LPV) magnitude on the distance between the contacts in the fabricated MOS structures exhibits a linear character. It was found that the maximum value of the lateral photovoltage increases significantly with increasing specific electrical resistivity in highly Zn-compensated n-type silicon samples. In particular, for the sample with ρ = 1800 Ω×cm, the maximum LPV reached ±16.83 mV at a distance of ±2.3 mm. This result demonstrates the high sensitivity of the LPE in structures based on highly compensated silicon. The obtained results are in good agreement with the energy band diagrams that consider the influence of deep energy levels associated with zinc atoms at the SiO₂/Si interface and the charge carrier concentration.
Keywords: *Lateral photoeffect; Highly compensated silicon; Metal-oxide-semiconductor structure; Lateral photovoltage; Interface states; Diffusion; Electron-beam evaporation; Thin film*

INTRODUCTION

The rapid development of science and technology in the modern era has significantly increased the demand for advanced materials with improved properties compared to existing ones. This trend has intensified the interest in the synthesis of new materials and the in-depth investigation of their physical characteristics. In particular, MOS structures play a crucial role in the development of modern nanoelectronics, high-sensitivity sensors, and position-sensitive detectors (PSDs) [1–3]. The LPE observed in MOS structures can be effectively utilized in the fabrication of PSDs [1–5]. The LPE is a phenomenon in which a photovoltage arises between the contacts when a focused light spot is incident on the semiconductor surface. The magnitude of this effect and its linear dependence on the distance between the contacts determine the accuracy and sensitivity of the detector.

In recent years, although the dependence of the LPE in MOS structures on the type and thickness of the metal and oxide layers has been relatively well investigated [2, 3, 5], its dependence on key semiconductor substrate parameters – such as the conductivity type, specific electrical resistivity, charge carrier concentration, and carrier mobility – remains insufficiently studied. In particular, the investigation of the LPE in MOS structures based on highly compensated silicon containing deep-level impurities is considered a highly relevant and topical issue.

Zinc (Zn) atoms, when diffused into silicon, create a series of deep acceptor and donor levels, significantly altering the electrophysical, recombination, and photoelectric properties of silicon [6, 7, 18]. As a result, highly compensated n-Si⟨P,Zn⟩ samples exhibit high specific resistivity (10^2–10^4 Ω×cm). Consequently, MOS structures fabricated on the basis of such samples can possess new functional properties.

The objective of this study is to develop the fabrication technology for Co/SiO₂/n-Si⟨P, Zn⟩ MOS structures and to experimentally determine how the resistivity of the semiconductor substrate affects the magnitude and sensitivity of the lateral photovoltage (LPV). Based on the above, the development of the fabrication technology for Co/SiO₂/n-Si⟨P, Zn⟩ MOS structures and the experimental study of the LPE in these structures, particularly the determination of the effect of specific resistivity on the magnitude and sensitivity of the LPV, are of significant scientific and practical importance. In this work, Co/SiO₂/n-Si⟨P⟩ and Co/SiO₂/n-Si⟨P, Zn⟩ MOS structures were synthesized on the basis of initial Silicone Electronic doped with Phosphorous (SEP-1).

Co/SiO₂/n-Si⟨P⟩ and Co/SiO₂/n-Si⟨P, Zn⟩ MOS Structure Fabrication Technology

To fabricate the Co/SiO₂/n-Si⟨P⟩ and Co/SiO₂/n-Si⟨P, Zn⟩ MOS structures, monocrystalline silicon (n-Si⟨P⟩) wafers doped with phosphorus atoms during crystal growth were initially used as substrates. The samples had dimensions of 8×4×1 mm³, a room-temperature resistivity of approximately 1 Ω×cm, and a crystallographic orientation of [111] along

Cite as: E.U. Arzikulov, R.M. Usanov, Sh.J. Quvondiqov, Teng Lui, D.T. Bobonov, S.A. Sattarov, East Eur. J. Phys. 3, 608 (2026), https://doi.org/10.26565/2312-4334-2026-3-56

the longitudinal direction. Subsequently, highly compensated n-Si⟨P, Zn⟩ samples exhibiting different conductivity types and a wide range of room-temperature electrical resistivities were synthesized. For the preparation of these samples, the high-temperature diffusion method was employed [19].

As is well known, the introduction of zinc atoms into silicon by the high-temperature diffusion method leads to the formation of acceptor levels with ionization energies of $E_v + 0.31$ eV and $E_v + 0.55$ eV. In addition, shallow acceptor levels with ionization energies of $E_v + 0.08$ eV, $E_i + 0.09$ eV, and $E_v + 0.13$ eV are formed, which are generally attributed to complexes of zinc atoms with Group III elements of the periodic table. In brief, the incorporation of zinc into silicon substantially alters its electrophysical, recombination, and photoelectric properties. As a result, highly compensated p(n)-Si<P, Zn> samples can be considered proMOSing novel materials for applications in modern micro- and nanoelectronics.

These same initial n-Si⟨P⟩ substrates (described above) were used for the diffusion process. Zinc with a purity of 99,96% was used as the diffusion source for introducing Zn atoms into the selected n-Si<P> samples. Using the temperature-dependent expressions for the diffusion coefficient and solubility of zinc in silicon, the diffusion temperature and duration required to obtain samples with different resistivities were determined in accordance with the procedure described in Ref. [19].

Highly compensated n-Si<P, Zn> samples were synthesized by the high-temperature diffusion method using a technique that takes into account the partial pressure of the diffusant vapor [20]. To remove the zinc-enriched surface layers formed during the high-temperature diffusion process, both mechanical and chemical treatment procedures were applied, and an average layer thickness of approximately 50 μm was removed from each side of the samples. As a result, relatively homogeneously doped, n-type, highly compensated n-Si<P, Zn> samples with room-temperature resistivities in the range of $10^2 \div 10^4$ Ω×cm were obtained. MOS structures were fabricated using the initial n-Si<P> samples, the n-Si<P> samples thermally annealed at the zinc diffusion temperature, and the synthesized highly compensated n-Si<P, Zn> samples. The primary objective of fabricating these structures was to distinguish and clarify the effects of thermal annealing and zinc incorporation on the measured characteristics.

The main parameters of the investigated samples before and after the diffusion process (electrical resistivity, mobility, and charge carrier concentration) were determined by Hall effect measurements. In this procedure, the native oxide layer on the initial samples and the zinc-enriched surface layers of the diffused samples were first removed. Subsequently, ohmic contacts were formed on the lateral sides of the samples using silver-based conductive adhesive. The corresponding measurements were then carried out as described in Ref. [9].

The parameters of the silicon samples before and after the diffusion process are presented in Table 1.

Table 1. Electrophysical parameters of the initial and Zn-diffused n-Si⟨P⟩ and n-Si⟨P, Zn⟩ samples before and after the diffusion process

Sample	ρ, Ω×cm	μ, $cm^2/(V \cdot s)$	n, cm^{-3}	Fermi level, eV
n–Si<P>, initial sample	1.05	1188.43	$5.01 \cdot 10^{15}$	0.254541
n–Si<P> (thermally annealed initial sample)	1.07	1167.32	$4.99 \cdot 10^{15}$	0.254659
n–Si<P, Zn>	5.04	650.8	$1.9 \cdot 10^{15}$	0.283144
n–Si<P, Zn>	156.86	690.26	$5.77 \cdot 10^{13}$	0.318301
n–Si<P, Zn>	1800	808	$4.28 \cdot 10^{12}$	0.39504

In the next stage, all samples whose parameters are presented in Table 2 were prepared for use as semiconductor substrates for the fabrication of MOS structures. The formation of the required oxide layer on the surface of these substrates was carried out in two steps. In the first step, the naturally formed oxide (SiO_2) layer resulting from various ambient processes was removed by immersing the samples in hydrofluoric acid (HF) for 15 s. The second step involved the growth of a silicon dioxide layer with a thickness of 2÷4 nm. This process was performed by immersing the samples (after the first step) in nitric acid (HNO_3) at a temperature of 121°C for 15 min [10]. It should be noted that oxidation in nitric acid is known to produce a relatively high density of oxide traps and interface states at the Si–SiO_2 interface [22].

After the formation of the SiO_2 oxide layer with the required thickness, a thin layer of metallic cobalt was deposited on top of it using electron-beam or thermal evaporation in vacuum, as well as magnetron sputtering techniques. The thickness of the metal layer was experimentally verified by spectroscopic ellipsometry. In this case, the oxide layer thickness was 3 nm, while the cobalt layer thickness was 10 nm.

For the investigation of the LFE in the synthesized Co/SiO_2/n-Si⟨P⟩ and Co/SiO_2/n-Si<P, Zn> MOS structures, the measurement setup described in Ref. [5] was used. The schematic diagram of the device is shown in Figure 1.

Since the magnitude of the LPV depends on parameters such as the charge carrier concentration and mobility in the semiconductor substrate, it was studied at optimal values of the metal and oxide layer thicknesses ($d_{ox} \approx 3$ nm, $d_m \approx 10$ nm). To measure the LPV, two point-like ohmic contacts were formed on the surface of the metal layer of all fabricated MOS structures using a conductive silver adhesive, as shown in Figure 1. A copper wire with a thickness of 50 μm was then placed onto this contact area, after which an additional layer of silver paste was applied and the structure was dried for 6 hours. After the silver paste had solidified, it was thermally treated using a Micro SET M RA laser welding system to ensure mechanical stability, resulting in a mechanically robust and reliable ohmic contact. The ohmicity of the

contacts was verified by measuring the current–voltage (I–V) characteristics between the contacts formed on the metal surface of the fabricated structures. Figure 1b presents the I–V characteristics of the thin Co layer in Co/SiO_2/n-Si<P, Zn> MOS structure based on an n-Si<P, Zn> substrate with a resistivity of 1800 Ω×cm. As can be seen, the dependence of the current flowing through the Co metal layer on the applied voltage between the surface contacts is linear.

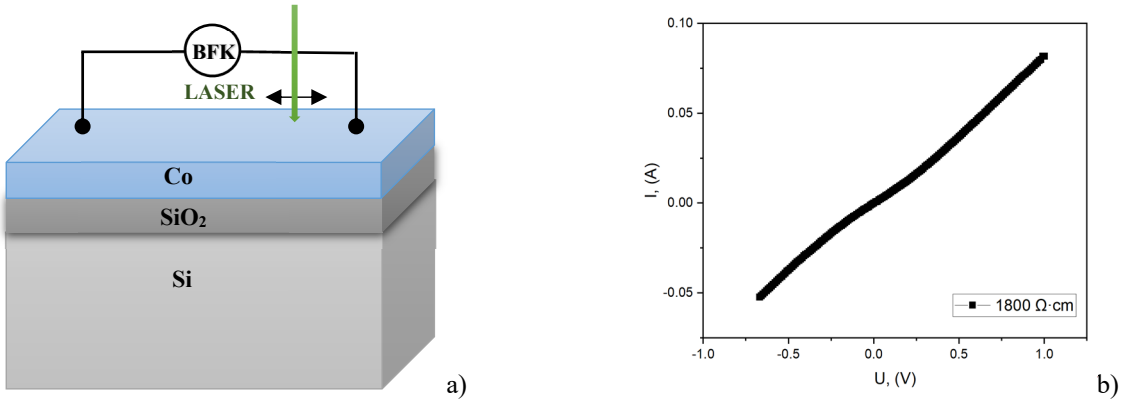

Figure 1. (a) Schematic view of the Co/SiO_2/n-Si hybrid structure and the measurement setup for lateral photovoltage, and (b) I–V characteristics of the metal layer of the Co/SiO_2/n-Si hybrid structure.

Experimental Results and Their Analysis

The I–V characteristics of the synthesized Co/SiO_2/n-Si<P> and Co/SiO_2/p(n)-Si<P, Zn> MOS structures were measured in the vertical direction with respect to the structure. In this configuration, one terminal of the external bias voltage source was connected to the ohmic contact formed on the thin metal film, while the other terminal was connected to the contact formed on the rear side of the semiconductor substrate. Subsequently, the polarity of the applied voltage source was reversed, and the I–V characteristics were measured again. The obtained results are presented in Figure 2.

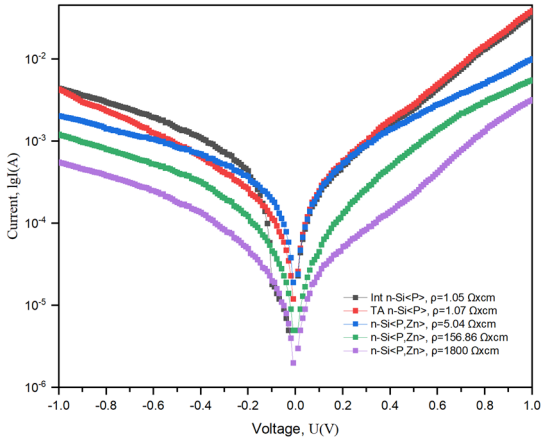

Figure 2. I–V characteristics of Co/SiO_2/n-Si<P> and Co/SiO_2/n-Si<P, Zn> MOS structures.

As can be seen from Figure 2, the I–V characteristics of the MOS structures fabricated on the initial samples, the samples annealed at the zinc diffusion temperature, and the samples with incorporated zinc atoms exhibit a typical behavior characteristic of such structures. Using the experimentally measured I–V characteristics of all synthesized Co/SiO_2/n-Si<P> and Co/SiO_2/n-Si<P, Zn> structures, the barrier height was calculated based on Refs. [11] and [12]. The calculated results are presented in Table 2.

Table 2. Schottky barrier heights of the Co/SiO_2/n–Si⟨P⟩ and Co/SiO_2/n–Si⟨P, Zn⟩ MOS structures, calculated from the I–V characteristics.

Q.s.	Structure	Resistivity of the Si substrate, Ω×cm	Potential barrier height, ϕ_B, eV
1	Co/SiO_2/n–Si<P> structure based on the initial sample	1.05	0.4734
2	Co/SiO_2/n–Si<P> structure based on the initial sample thermally annealed at 1150°C	1.07	0.4722
3	Co/SiO_2/n–Si<P, Zn> structure	5.04	0.4378
4	Co/SiO_2/n–Si<P, Zn> structure	156.86	0.5463
5	Co/ SiO_2/n–Si<P, Zn> structure	1800	0.4798

As can be seen from Table 2, a well-defined potential barrier is formed in the investigated samples. The differences in the barrier height values observed in the Co/SiO_2/n-Si<P, Zn> structures may be associated with the modification of impurity-induced surface states formed by zinc atoms, as well as changes in the charge states at the SiO_2/n-Si<P, Zn> interface.

Surface condition has a significant impact on the electrical parameters of MOS structures. Therefore, we studied the surface condition of a pure semiconductor substrate, a substrate with a tunnel-thin oxide layer, and a substrate with a thin metallic cobalt layer at room temperature using an FusionScope Scanning Electron Microscope (SEM). This modern SEM microscope allows for surface examination of substrates in both SEM and Atomic Force Microscopy (AFM) modes. The results are shown in Figure 3.

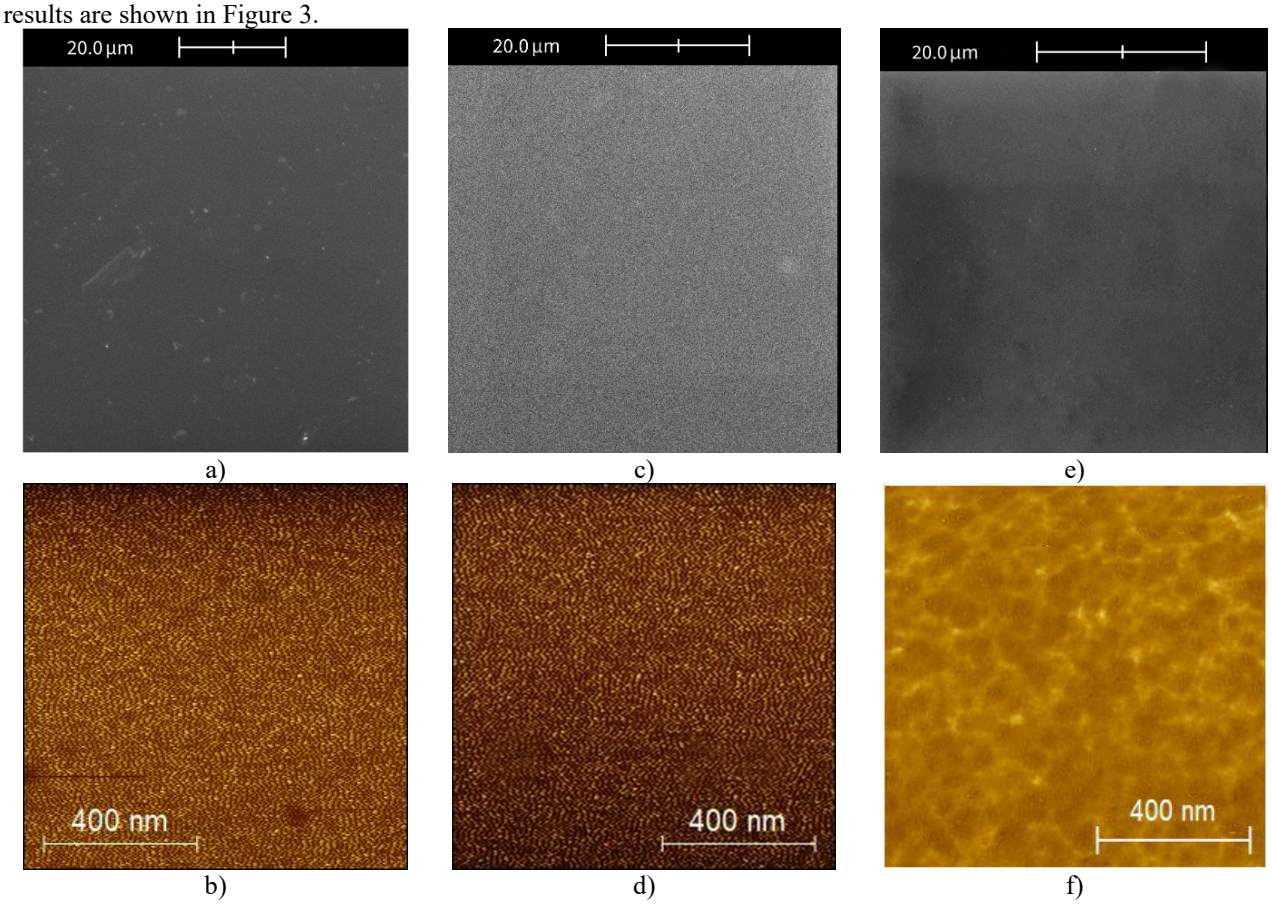

Figure 3. SEM and AFM images of the Co/SiO_2/n-Si hybrid structures: (a, b) initial silicon surface; (c, d) silicon surface after chemical cleaning; (e, f) SEM and AFM images of the cobalt thin films.

Figure 3 presents the surface morphology of the Co/SiO_2/n-Si hybrid structures at three critical stages: the initial state, post-chemical cleaning, and following the deposition of the Co thin film, as characterised by Scanning Electron Microscopy (SEM) and Atomic Force Microscopy (AFM). Figures 3(a) and 3(b) display the surface of the initial silicon substrate. The SEM micrograph (Figure 3a) reveals the presence of residual macroscopic particulate contaminants on the uncleaned surface. Corroborating this observation, the AFM topographical analysis (Figure 3b) demonstrates an initial root-mean-square (RMS) surface roughness (R_q) of 59.19 nm. Following the chemical cleaning procedure, a drastic morphological improvement is observed. The SEM image in Figure 3(c) shows the successful elimination of the surface impurities, yielding a highly pristine and uniform silicon surface. The corresponding AFM image (Figure 3d) confirms this planarization, exhibiting a substantial decrease in the surface roughness to 2,42 nm, thereby validating the efficacy of the chemical treatment. Figures 3(e) and 3(f) illustrate the surface characteristics after the Co thin film deposition. While the macroscopic SEM image (Figure 3e) suggests the formation of a highly smooth and uniform Co layer with an apparent roughness of 2.69 nm, the high-resolution AFM topography (Figure 3f) provides a deeper insight into the nanoscale growth dynamics. The AFM image reveals that the Co layer forms via the Volmer-Weber (island) [21] growth mechanism, characterised by discrete nanostructured formations. In the regime of ultra-thin metallic films, this island-like morphology plays a pivotal role in determining the electrical transport properties of the structure. The discrete granular nature of the film significantly enhances conduction electron scattering at the boundaries of these islands, which leads to a pronounced increase in the sheet resistance (R_s) of the metal layer.

The dependence of the measured LPV on the distance between the contacts in Co/SiO_2/n-Si<P> and Co/SiO_2/p-Si<P, Zn> MOS structures is shown in Figure 4.

As can be seen from the figure, in all investigated structures the dependence of the LPV on the distance between the contacts exhibits an approximately quasi-linear behavior.

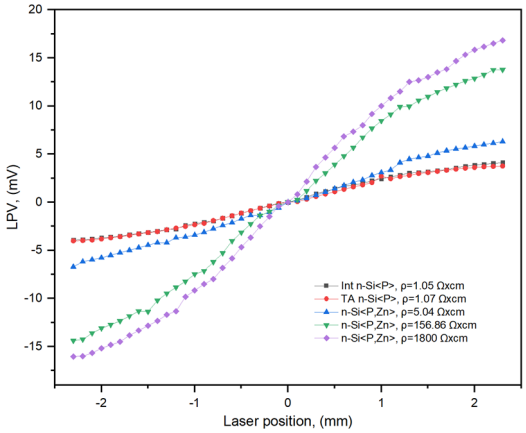

Figure 4. Dependence of the LPV magnitude on the laser beam position

To evaluate the linearity of such dependences, the nonlinearity coefficient δ and the correlation coefficient r, defined by the following expressions, are used [3].

$$Nonlinearity = \delta = \frac{2\times RMS}{maximum\ value\ of\ LPV}, \tag{1}$$

here, RMS denotes the standard deviation (root mean square deviation), and r is the correlation coefficient

$$y - \bar{y} = r\frac{\sigma_y}{\sigma_x}(x - \bar{x}), \tag{2}$$

where $\sigma_x, \sigma_y -$ are the standard (root mean square) deviations.

In addition, the sensitivity coefficient k, which determines the practical applicability of the investigated structures and is defined by the following expression, is calculated using Eq. (3):

$$k = \frac{d(LPV)}{dx}. \tag{3}$$

Under the given experimental conditions, it was found that the maximum LPV value in Co/SiO₂/n-Si<P>-based MOS structures strongly depends on the resistivity of the semiconductor substrate. In particular, in the initial and thermally treated Co/SiO₂/n-Si<P> samples with relatively low resistivity, the maximum LPV values were comparatively small, amounting to ±4.11 mV and ±3.76 mV, respectively. At the same time, in Co/SiO₂/n-Si<P, Zn> samples, the maximum LPV value increased significantly with increasing resistivity. For samples with resistivities of 5.04 Ω×cm, 156.86 Ω×cm, and 1800 Ω×cm, the corresponding LPV maxima reached ±6.31 mV, ±13.77 mV, and ±16.83 mV, respectively.

The values of the parameters related to nonlinearity for the dependence of the LPV on the distance between contacts in the synthesized Co/SiO₂/n-Si<P> and Co/SiO₂/p-Si<P, Zn> MOS structures, i.e., the quantities defined by Eqs. (1)-(3), were calculated based on the experimental results. The obtained calculation results are presented in Table 3.

Table 3. Position sensitivity (k), Correlation coefficient (r), and nonlinearity (δ) coefficients of the LPV response for the investigated Co/SiO₂/n–Si⟨P⟩ and Co/SiO₂/n–Si⟨P, Zn⟩ MOS structures

Sample	ρ, Ω×cm	k, mV/mm	r	δ, %
Co/SiO₂/n–Si<P>	1.05	1.9966	0.9944	7.18
Co/SiO₂/n–Si<P>	1.07	1.9504	0.9950	7.34
Co/SiO₂/p–Si<P,Zn>	5.04	2.9929	0.9976	4.43
Co/SiO₂/p–Si<P,Zn>	156.86	6.8451	0.9961	5.84
Co/SiO₂/p–Si<P,Zn>	1800	8.1887	0.9943	7.25

Within the scope of this study, the effect of the semiconductor substrate resistivity on the position sensitivity characteristics of Co/SiO₂/n-Si<P> and Co/SiO₂/p-Si<P, Zn> MOS structures was investigated. The obtained experimental results demonstrate that with an increase in resistivity, the position sensitivity coefficient k of the device increases from 1.9966 mV/mm to 8.1887 mV/mm. This behavior can be explained by the redistribution of charge carriers in high-resistivity samples.

The fact that the correlation coefficient r for all samples lies in the range 0,9943÷0,9976 confirms a sufficiently high degree of linearity between the LPV values and the coordinate. This represents an important advantage for the potential application of MOS structures as position-sensing devices.

The nonlinearity degree δ was found to vary in the range of 4.43% to 7.34%, remaining within the accepted technological criterion (δ < 15%) [13] in all cases. At the same time, the minimum nonlinearity value (4.43%) was observed for the sample with a resistivity of 5.04 Ω×cm, indicating an optimal operating regime of the device in this range. Although high-resistivity samples provide higher sensitivity, they are also characterized by a slight increase in nonlinearity, which indicates a trade-off between sensitivity and accuracy.

DISCUSSION OF EXPERIMENTAL RESULTS

To explain the obtained results from a physical point of view, the energy band diagrams of the investigated Co/SiO_2/n-Si<P> and Co/SiO_2/n-Si<P, Zn> structures were constructed theoretically in analogy with Ref. [4].

In a Me/SiO_2/Si structure, when the metal film is non-uniformly illuminated, the transmitted light generates electron–hole pairs in the illuminated region of silicon. These carriers then diffuse toward the existing space-charge region in silicon and are separated by the internal electric field of the structure. The magnitude and direction of this field depend on the value and sign of the built-in potential barrier $q\varphi_i$. This potential is determined by the difference between the work functions of the metal and silicon. It should be noted that the electron work function of silicon depends on the type and concentration of the doping impurity.

In this study, we used semiconductor substrates fabricated from industrial SEP-1 silicon, doped with phosphorus during crystal growth, as well as highly compensated n-Si<P, Zn> samples obtained by high-temperature diffusion. The electron work function of silicon can be estimated by the following equation:

$$q\varphi_s = q\chi_{Si} + (E_F - E_C), \tag{4}$$

here $q\chi_{Si} = 4.05\ eV$ −is the electron affinity of silicon, and $E_F - E_C$ − is the energy distance between the Fermi level and the conduction band edge. For the n-Si<P> case, $E_F - E_C$ − is determined by the expression: $E_F - E_C = kTln(N_C/N_D)$ where N_C is the effective density of states at the conduction band edge, which at 300 K is $N_C = 2.8 \cdot 10^{19}\ cm^{-3}$ [8], and N_D is the electron concentration in the sample at room temperature. For the n-Si<P> (111) sample with resistivity ρ = 1.05 Ω×cm, the donor concentration is $N_D = 5.01 \cdot 10^{15} cm^{-3}$ and $E_F - E_C = 0.22\ eV$. Accordingly, the electron work function is found to be 4.27 eV.

Similarly to the n-Si<P> sample, for n-Si<P, Zn> (111) samples with resistivities of ρ = 5.04, 156.86, and 1800 Ω×cm, the donor (electron) concentrations are $N_D = 1.9 \cdot 10^{15};\ 5.77 \cdot 10^{13};\ 4.28 \cdot 10^{12} cm^{-3}$, respectively. The corresponding values of $(E_F - E_C)$ are found to be 0.28 eV, 0.39 eV, and 0.46 eV.

For the energy band diagram of the Co/SiO_2/n-Si<P, Zn> structure, the following values can be obtained. For example, for an n-Si<P, Zn> sample with a room-temperature resistivity of ρ = 1800 Ω×cm, the donor concentration is $N_D = 4.28 \cdot 10^{12} cm^{-3}$ and $E_F - E_C = 0.46$. Consequently, the electron work function for this sample is 4.51 eV. Using the same approach, the electron work functions for the remaining n-Si<P, Zn> samples are found to be 4.33 eV and 4.44 eV, respectively.

Taking into account that the electron work function of cobalt is 4,40 eV, the resulting potential values in n-Si<P> and n-Si<P, Zn> samples are found to be 0.13 eV, 0.07 eV, −0.04 eV, and −0.06 eV, respectively. In the initial samples and in the n-Si<P, Zn> structure with a resistivity of 5.05 Ω·cm, the energy bands at the SiO_2/Si interface are bent upward, and the resulting internal electric field is directed from silicon toward the cobalt film.

Based on these data, the equilibrium band diagrams of the Co/SiO_2/n-Si<P> and Co/SiO_2/n-Si<P, Zn> structures were constructed, as shown in Figure 6. The analysis of the band diagrams indicates that in the Co/SiO_2/n-Si<P> structure, and in the Co/SiO_2/n-Si<P, Zn> structure with a resistivity of 5.05 Ω×cm, the upward band bending is more pronounced compared to the Co/SiO_2/n-Si<P, Zn> structures. In this case, $\varphi_S = E_i(0) - E_i = 0.13\ eV$ and $\varphi_F = E_F - E_i = 0.22\ eV$, and since $\varphi_S < \varphi_F$, an accumulation layer is formed at the SiO_2/Si interface instead of an inversion layer. In contrast, in Co/SiO_2/n-Si<P, Zn> structures with resistivities of 156.86 and 1800 Ω×cm, the bands are bent downward, leading to the formation of a depletion layer at the SiO_2/Si interface (Figure 6b). In this case, the internal electric field is directed from the thin cobalt film toward the silicon substrate. This, in turn, results in the drift of photogenerated holes toward the SiO_2/Si interface in the initial Co/SiO_2/n-Si<P> structure and in the Co/SiO_2/n-Si<P, Zn> structure with 5.05 Ω×cm resistivity, whereas in the Co/SiO_2/n-Si<P, Zn> structures with resistivities of 156,86 and 1800 Ω×cm, electrons are attracted toward this interface.

Figures 6(a) and 6(b) show the energy band diagrams of the Co/SiO_2/n-Si<P> and Co/SiO_2/n-Si<P, Zn> structures, respectively, taking into account interface states.

These figures clearly show that, for Co/SiO_2/n-Si<P, Zn> structures with resistivities of 156.86 and 1800 Ω×cm, taking into account interface states leads to negative potential values ($q\varphi_i = -0.04\ eV\ and\ -0.06\ eV$, respectively) and a reversal of the band bending direction. As a result, a depletion n-type layer is formed at the SiO_2/Si interface. The direction of the electric field is also reversed, so that, unlike the ideal case, photogenerated holes rather than electrons are attracted toward the SiO_2/Si interface. For the Co/SiO_2/n-Si<P> structure, the band bending is reduced to about 0.03 eV, and, as in the ideal case, no inversion layer is formed at the SiO_2/Si interface (as shown in Figure 6a), where $\varphi_S = 0.13\ eV$, $\varphi_F = 0.22\ eV$ and $\varphi_S < \varphi_F$. Thus, considering only interface states at the SiO_2/Si boundary leads to different directions

of the internal electric field in Co/SiO₂/n-Si<P> and Co/SiO₂/n-Si<P, Zn> structures, which in turn results in corresponding changes in the current transport mechanisms in the investigated structures.

As can be seen from Figure 4, under the given conditions, the observed maximum value of the LPV in the Co/SiO₂/p-Si<P, Zn> structure is approximately four times higher than that in the Co/SiO₂/n-Si<P> structure.

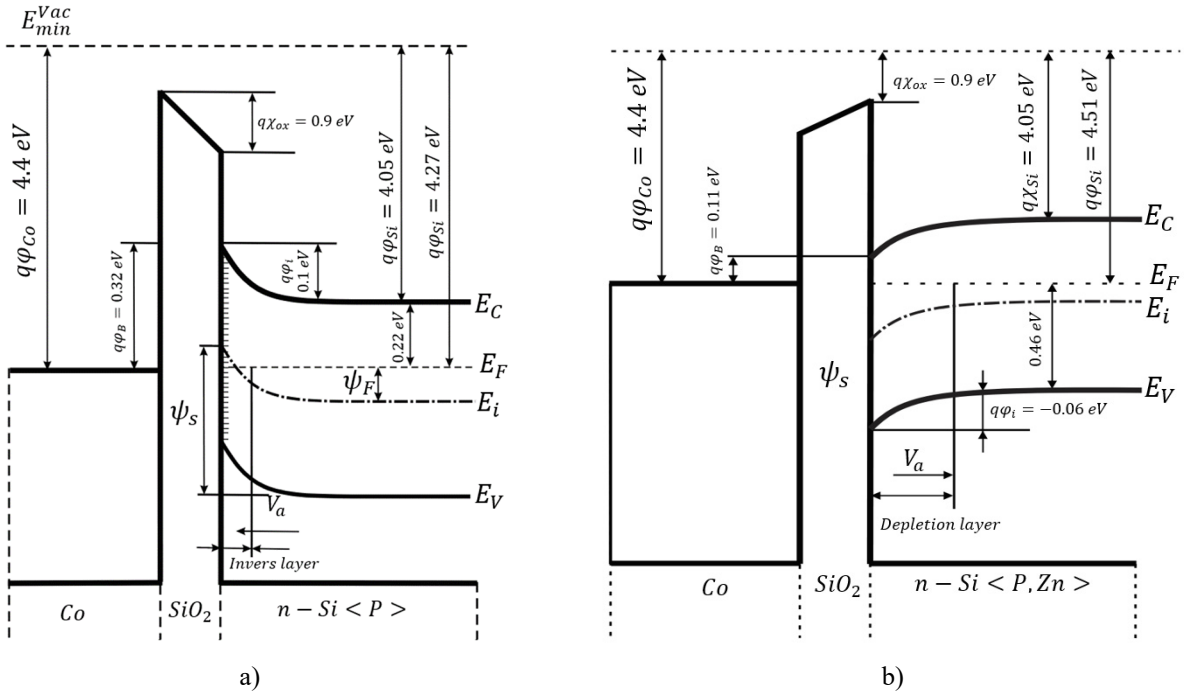

Figure 6. Energy band diagrams of Co/SiO₂/n-Si<P> (a) and Co/SiO₂/n-Si<P, Zn> (b) structures at the SiO₂/Si interface, taking into account interface states

These values correspond to the ohmic contact region and show a significant deviation from the results reported for similar structures investigated in other studies [2]. Such a pronounced difference in the results may be attributed to several factors. The first possible reason is the difference in the laser beam power used in our study and in other works [2,3] on LPV investigation. The LPV value strongly and nonlinearly depends on the incident laser power; in particular, an increase in laser power leads to an increase in LPV, which can cause significant discrepancies between the measured values in different studies. The second reason may be the differences in the thicknesses of the oxide and metal layers in the investigated structures. These layer thicknesses have a strong influence on the LPV magnitude [2]. The third reason may be the differences in the semiconductor substrate parameters used in the fabrication of the structures, such as charge carrier concentration and mobility, as well as the differences in interface states at the SiO₂/Si boundary compared to those reported in other studies [4]. All the factors mentioned above may lead to significant differences in the obtained experimental results.

When the structure is illuminated, the reduction of the potential barrier is determined by the following expression [4]:

$$qV_a = kT\ln\left[1 + \frac{F_0}{sn_0}\left(1 - \frac{\exp(-\alpha d)}{1+\alpha L_{eff}}\right)\right], \tag{5}$$

here k is the Boltzmann constant, T is the temperature, q is the electron charge, F_0 is the photon flux density incident on the silicon surface, $s = \vartheta_T/4$ (where $\vartheta_T -$ is the average thermal velocity of charge carriers), $n_0 -$ is the concentration of majority carriers at the SiO₂/n-Si interface under dark conditions, $\alpha -$is the optical absorption coefficient, $d -$is the space-charge region width, and $L_{eff} -$ is the effective diffusion length of minority carriers. By substituting the values of the majority carrier concentration at the SiO₂/Si interface for the Co/SiO₂/n-Si<P> and Co/SiO₂/n-Si<P, Zn> structures into Eq. (1), the following approximately values of qV_a are obtained: ~$1.34\cdot10^{-9}$ eV and ~$2.21\cdot10^{-9}$ eV, respectively.

As noted above, in Co/SiO₂/n-Si<P> and Co/SiO₂/n-Si<P, Zn> structures, a linear relationship between the laser spot position and the lateral photovoltage is observed in some cases, while in other structures an exponential decay behavior is also present. Such dependences can be explained by the fact that the metal film on the structure surface serves only to induce band bending in the silicon near the SiO₂/Si interface, whereas the LPV generation process takes place in the near-surface region of silicon. Depending on the degree of band bending, accumulation, depletion, or inversion layers are formed in the subsurface region of silicon, leading to the formation of p–n, p^-–n–, (n^-–n) or p^+–n, (n^+–n), etc. junctions, to which the theory of the LPV effect can be applied. For example, in the Co/SiO₂/n-Si<P> structure, an inversion layer and a p–n junction formed by the silicon bulk are created at the SiO₂/Si interface. In this case, excess photogenerated

carriers act as majority carriers in both p- and n-type regions. For this structure, the diffusion theory of the LPV effect, based on the continuity equation of the total current of majority carriers and the linear dependence of LPV on the light spot position, can be derived and is given in the following form [4]:

$$LPV = K_1\left[e^{\beta|\varphi_i|}\right](|x_1| - |x_2|), \quad (6)$$

Here K_1 – is the proportionality coefficient, β=q/(kT), φ_i – is the built-in potential, and x_1, x_2 – are the distances from the illumination point to the contacts. From Eq. (6), it can be seen that the magnitude of the LPV increases exponentially with an increase in the generated potential and becomes zero at the midpoint between the contacts (i.e., when $x_1 = x_2$), exhibiting a linear variation across the contact spacing. This behavior is experimentally observed in Co/SiO_2/n-Si<P> and Co/SiO_2/n-Si<P, Zn> structures, as shown in Figure 4.

CONCLUSIONS

In this study, Zn atoms were introduced into initial KEF-1 n-Si⟨P⟩ samples (ρ ≈ 1.05 Ω×cm) using a high-temperature diffusion method, resulting in the synthesis of strongly compensated n-Si⟨P, Zn⟩ samples with various resistivity levels (ρ = 5.04, 156.86, and 1800 Ω×cm). Based on these substrates, Co/SiO_2/n-Si⟨P, Zn⟩ MOS structures were fabricated, and a reproducible technology for their preparation was developed.

Based on the obtained results, it can be concluded that by optimizing the resistivity of the semiconductor substrate in Co/SiO_2/n-Si<P, Zn> MOS structures, it is possible to develop position-sensitive devices with high sensitivity. These findings broaden the prospects for the application of MOS-based PSD devices in optoelectronic and sensor systems requiring high precision.

In Co/SiO_2/n-Si⟨P, Zn⟩ MOS structures, an increase in the resistivity of the n-Si⟨P, Zn⟩ substrate has a significant influence on the fundamental physical mechanisms of the LPV effect. The experimental results showed that the dependence of LPV on the distance between contacts exhibits a highly accurate linear behavior in the fabricated structures. With increasing resistivity, a substantial increase in the maximum LPV value was observed. In particular, the maximum LPV value of ±4.11 mV in the initial n-Si⟨P⟩ samples increased to ±16.83 mV in the highly compensated sample with ρ = 1800 Ω×cm, corresponding to an approximately fourfold enhancement. At the same time, the position sensitivity coefficient increased from k = 1.9966 V/mm to 8.1887 V/mm. The correlation coefficient ranged within r = 0.9943–0.9976, confirming a high degree of linearity, while the nonlinearity remained within δ = 4.43–7.34%, fully satisfying the accepted technological criterion (δ < 15%).

The obtained results are in good agreement with the energy band diagrams constructed by taking into account the interface states at the SiO_2/Si boundary and the redistribution of charge carrier concentration. In MOS structures fabricated on strongly compensated (high-resistivity) silicon substrates obtained via Zn diffusion, an efficient formation of the internal electric field and redistribution of charge carriers occur, which leads to a significant enhancement of LPV sensitivity.

The results of this study demonstrate the potential application of MOS structures based on Zn-high compensated n-Si⟨P, Zn⟩ as proMOSing materials for the development of position-sensitive detectors (PSDs), high-precision optoelectronic sensors, and nanoelectronic devices. Furthermore, these findings establish a scientific basis for designing high-sensitivity, high-linearity, and high-accuracy devices by further tailoring the semiconductor substrate resistivity and interface states in MOS structures.

It is worth noting that some commercially available position-sensitive detectors, as well as certain devices reported in the literature, reportedly employ silicon substrates with considerably higher resistivity than the maximum investigated in the present work. It should be emphasized, however, that the present study already covers a broad resistivity range — from ~1 Ω×cm in the initial n-Si ⟨P⟩ samples to 1800 Ω×cm in the highly Zn-compensated samples; extending this range toward even higher resistivities represents a promising direction for future research. It is also worth noting that, based on the physical mechanism underlying the LPE, deep-level-compensated silicon substrates such as those used in this study are expected to provide considerably higher LPV sensitivity than nominally pure (uncompensated) high-resistivity silicon of comparable resistivity, owing to the more efficient formation of the internal electric field associated with deep-level compensation; a direct experimental comparison between the two substrate types remains an interesting subject for future work. In addition, since the SiO_2 layer in this work was formed by oxidation in nitric acid, exploring alternative oxidation methods to further reduce interface-state density and improve device performance represents another promising direction for our future research.

ORCID

E.U. Arzikulov, https://orcid.org/0000-0001-9179-3402; **R.M. Usanov,** https://orcid.org/0000-0003-2738-7535

REFERENCES

[1] Wallmark, J. "A New Semiconductor Photocell Using Lateral Photoeffect," Proc. IRE, **45**, 474–483 (1957). https://doi.org/10.1109/JRPROC.1957.278435

[2] Xiao, S.Q., Wang, H., Zhao, Z.C., Gu, Y.Z., Xia, Y.X., and Wang, Z.H. "The Co-Film-Thickness Dependent Lateral Photoeffect in Co-SiO_2-Si Metal-Oxide-Semiconductor Structures," Opt. Express, **16**, 3798 (2008). https://doi.org/10.1364/OE.16.003798

[3] Xiao, S.Q., Wang, H., Yu, C.Q., Xia, Y.X., Lu, J.J., Jin, Q.Y., and Wang, Z.H. "A Novel Position-Sensitive Detector Based on Metal–Oxide–Semiconductor Structures of Co–SiO_2 –Si," New J. Phys. **10**, 033018 (2008). https://doi.org/10.1088/1367-2630/10/3/033018
[4] T.A. Pisarenko, V.V. Balashev, V.A. Vikulov, A.A. Dimitriev, and V.V. Korobtsov, "Comparative Study of the Lateral Photovoltaic Effect in Fe_3O_4/SiO_2/n-Si and Fe_3O_4/SiO_2/p-Si Structures," Phys. Solid State, **60**, 1316–1322 (2018). https://doi.org/10.1134/S1063783418070223
[5] Arzikulov, E.U., Nurimov, A.D., Salakhitdinov, F.A., Ashirov, U.A., Sharafova, T.S., Khujanov, A.Sh., Usanov, R.M., "Lateral Photoelectric Effect In Iron-Silicon Dioxide-Compensated Silicon Hybrid Structures," East Eur. J. Phys. (4), 159–166 (2023). https://doi.org/10.26565/2312-4334-2023-4-17
[6] Fuller, C.S., and Morin, F.J., "Diffusion and Electrical Behavior of Zinc in Silicon," Phys. Rev. **105**, 379–384 (1957). https://doi.org/10.1103/PhysRev.105.379
[7] R.O. Carlson, "Double-Acceptor Behavior of Zinc in Silicon," Phys. Rev. **108**, 1390–1393 (1957). https://doi.org/10.1103/PhysRev.108.1390
[8] S.M. Sze, and K.K. Ng, *Physics of Semiconductor Devices*, 3rd ed. (Wiley-Interscience, Hoboken, N.J, 2007).
[9] E.V. Kuchis, *Galvanomagnetic Effects and Methods of Their Investigation*, (Radio i Svyaz Publishers, Moscow, 1990).
[10] H. Angermann, "Conditioning of Si-Interfaces by Wet-Chemical Oxidation: Electronic Interface Properties Study by Surface Photovoltage Measurements," Appl. Surf. Sci. **312**, 3–16 (2014). https://doi.org/10.1016/j.apsusc.2014.05.087
[11] A.R. Deniz, Z. Çaldıran, Ö. Metin, K. Meral, and Ş. Aydoğan, "The Investigation of the Electrical Properties of Fe_3O_4/n-Si Heterojunctions in a Wide Temperature Range," J. Colloid Interface Sci. **473**, 172–181 (2016). https://doi.org/10.1016/j.jcis.2016.04.006
[12] S.K. Cheung, and N.W. Cheung, "Extraction of Schottky Diode Parameters from Forward Current-Voltage Characteristics," Appl. Phys. Lett. **49**, 85–87 (1986). https://doi.org/10.1063/1.97359
[13] E. Fortunato, G. Lavareda, R. Martins, F. Soares, and L. Fernandes, "Large-Area 1D Thin-Film Position-Sensitive Detector with High Detection Resolution," Sens. Actuators Phys. **51**, 135–142 (1995). https://doi.org/10.1016/0924-4247(95)01214-1
[14] R. Cong, S. Qiao, J. Liu, J. Mi, W. Yu, B. Liang, G. Fu, *et al*., "Ultrafast, and Self-Powered Visible-Near-Infrared Optical Position-Sensitive Detector Based on a CVD-Prepared Vertically Standing Few-Layer MoS_2 /Si Heterojunction," Adv. Sci. **5**, 1700502 (2018). https://doi.org/10.1002/advs.201700502
[15] X. Dong, D. Zheng, J. Lu, Y. Niu, and H. Wang, "Selectively Enhanced Violet and Infrared Position Sensitive Photodetectors Based on RTA Treated ZnO/Si," Appl. Surf. Sci. **566**, 150687 (2021). https://doi.org/10.1016/j.apsusc.2021.150687
[16] X. Wang, B. Song, M. Huo, Y. Song, Z. Lv, Y. Zhang, Y. Wang, *et al*., "Fast and Sensitive Lateral Photovoltaic Effects in Fe_3O_4/Si Schottky Junction," RSC Adv. **5**, 65048–65051 (2015). https://doi.org/10.1039/C5RA11872G
[17] J.R. Sun, C.M. Xiong, B.G. Shen, P.Y. Wang, and Y.X. Weng, "Manganite-Based Heterojunction and Its Photovoltaic Effects," Appl. Phys. Lett. **84**, 2611–2613 (2004). https://doi.org/10.1063/1.1702128
[18] M.K. Bakhadyrkhanov, N.F. Zikrillaev, and E.U. Arzikulov, "Influence of diffusant vapor pressure on the concentration of electroactive atoms and the degree of compensation in Si⟨Zn⟩ samples," Pis'ma v ZhTF, **17**(12). 1–4 (1991). (in Russian)
[19] M.K. Baxadirxanov, N.F. Zikrillayev, and E.U. Arzikulov, "Vliyaniye uprugosti parov diffuzanta na konsentrasiyu elektroaktivnыx atomov i stepen kompensasii obrazsov Si⟨Zn⟩," Pisma v JTF, **17**(12), 1–4 (1991). (in Russian)
[20] Q.S. Ayupov, M.K. Baxadirxanov, N.F. Zikrillaev, and X.M. Iliev, *Physical phenomena in silicon in an extremely non-equilibrium state*, (Lambert Academic Publishing, 2019).
[21] Y. Shiratsuchi, T. Murakami, Y. Endo, and M. Yamamoto, "Evolution of Magnetic State of Ultrathin Co Films with Volmer–Weber Growth," Jpn. J. Appl. Phys. **44**(12R), 8456 (2005). https://doi.org/10.1143/JJAP.44.8456
[22] H.K. Asuha, O. Maida, M. Takahashi, and H. Iwasa, "Nitric acid oxidation of Si to form ultrathin silicon dioxide layers with a low leakage current density," J. Appl. Phys. **94**(11), 7328–7335 (2003). https://doi.org/10.1063/1.1621720

ЛАТЕРАЛЬНИЙ ФОТОЕФЕКТ У СТРУКТУРАХ МЕТАЛ–ОКСИД–НАПІВПРОВІДНИК НА ОСНОВІ МОНОКРИСТАЛІЧНОГО КРЕМНІЮ

Е.У. Арзікулов[1,2], Р.М. Усанов[1], Ш.Дж. Кувондіков[1], Тенг Луй[1,2], Д.Т. Бобонов[3], С.А. Саттаров[1,3]
[1]Самаркандський державний університет імені Шарофа Рашидова,
140001, Університетський бульвар, 15, Самарканд, Узбекистан
[2]Школа матеріалознавства та інженерії, Шеньянський аерокосмічний університет,
проспект Даої Саут, 37, Шеньян, Китай
[3]Джизакський політехнічний інститут, Джизак, Узбекистан

У цій статті представлено технологію виготовлення та експериментальні результати дослідження латерального фотоефекту (ЛФЕ) в метал-оксид-напівпровідникових (МОП) структурах Co/SiO_2/n-Si⟨P, Zn⟩. Структури були виготовлені на основі вихідних зразків кремнію n-типу (ρ=1,05 Ом×см), термічно відпалених зразків (ρ=1,07 Ом×см) та висококомпенсованих Zn зразків кремнію n-типу з питомим опором 5,04 Ом×см, 156,86 Ом×см та 1800 Ом×см відповідно. Згідно з експериментальними результатами, залежність величини латеральної фото-ерс (ЛФЕ) від відстані між контактами у виготовлених МОН-структурах має лінійний характер. Було виявлено, що максимальне значення латеральної фото-ерс значно зростає зі збільшенням питомого електричного опору у висококомпенсованих Zn зразках кремнію n-типу. Зокрема, для зразка з ρ = 1800 Ом×см максимальне ЛФЕ досягло ±16,83 мВ на відстані ±2,3 мм. Цей результат демонструє високу чутливість ЛФЕ в структурах на основі висококомпенсованого кремнію. Отримані результати добре узгоджуються з діаграмами енергетичних зон, які враховують вплив глибоких енергетичних рівнів, пов'язаних з атомами цинку на межі розділу SiO_2/Si, та концентрацію носіїв заряду.

Ключові слова: *латеральний фотоефект; висококомпенсований кремній; структура метал-оксид-напівпровідник; латеральна фотоенергія; стани на межі розділу; дифузія; електронно-променеве випаровування; тонка плівка*